5-(2-Carboxyethenyl)-Isatin Derivatives as Anticancer Agents: QSAR, Molecular Docking and Molecular Dynamic Simulation Analysis

L. Emami[1,2], Z. Faghih[1] *, M. Fereidoonnezhad[3], S. Khabnadideh[1,2],
F. Salehi[2], A. Abbasi[1,2], A.H. Sakhteman[2]

[1] *Pharmaceutical Sciences Research Center, Shiraz University of Medical Sciences, Shiraz, Islamic Republic of Iran*
[2] *Department of Medicinal Chemistry, Faculty of Pharmacy, Shiraz University of Medical Sciences, Shiraz, Islamic Republic of Iran*
[3] *Department of Medicinal Chemistry, School of Pharmacy, Ahvaz Jundishapur University of Medical Sciences, Ahvaz, Islamic Republic of Iran*

Abstract

Isatin and its analogues have been shown anticancer activity against various cancer cell lines via restrainting cancer cell proliferation and tumor growth. In this study, five different statistical methods such as MLR, PCR, FA-MLR, GA-MLR, and GA-PLS, were used to aquaire the Quantitative relevance between cytotoxicity activity and 37 isatin structures. Quantitative structure activity models indicated that topological and gateway parameters have an adequate impact on the cytotoxic activity of the tested molecules. Among the applied QSAR models, GA-PLS and MLR gave significant results with high statistical quality for predicting the inhibitory activity of the molecules. Molecular docking studies of these compounds were also investigated, and promising results were obtained. There was a good correlation between QSAR and docking results. For the validity of the docking studies, molecular dynamics (MD) simulation was also done.

Keywords: Isatin; Anticancer; MD simulation; QSAR; Docking.

Introduction

Cancer is a genetic disorder disease involving abnormal cell growth to attack and spread to other parts of the body. Cancer is also the second most common cause of mortality after cardiovascular disease in developed countries and is the third most common cause of death in other countries. According to the WHO global cancer report 2014, it is expected to increase by 57% worldwide in the next 20 years [1]. By 2030, it is projected that there will be 26 million new cancer cases and 17 million cancer deaths per year [2, 3]. The projected increase will be driven mainly cause by growth and aging populations and will be most significant in low-resource and medium-resource countries [4].

Isatin and its analogues possess a wide spectrum of activities including antimicrobial [5, 6], antitumor [7-

11], antiviral [12], anti-inflammatory [13], and antioxidant activities [14]. The isatin containing heterocycles can also act as inhibitors of apoptosis [15], targeting proteases [16], caspases [17], kinases [18], and extracellular signal-regulated protein kinase (ERK) [19].

Expression of pharmalogical activities by quantitative assessments are so important in medicinal chemistry and drug discovery. [20]. The correlation between variation of biological properties and molecular structures, is considered as an essential approach for understanding the mechanism of action of drugs and designing new ones.

There are various variable selection methods including multiple linear regression (MLR), principal component or factor analysis (PCA/FA), genetic algorithm (GA), and so on available for QSAR studies [21].

Here, QSAR studies of novel series of 5-(2-Carboxyethenyl)-isatin derivatives as anticancer compounds which have been designed and synthesized recently by Teng Yu-Ou [22] have been explored. To stablish the relationship betwean structural features of the compounds and their inhibitory activity on Jurkat cells proliferation, different statistical methods were applied. These methods included: (i) multiple linear regression (MLR), (ii) genetic algorithm-partial least squares (GA-PLS), (iii) MLR with factor analysis as the data pre-processing step for variable selection (FA-MLR), and (iv) principal component regression (PCR). These thirty-seven compounds were also used to investigate the detailed molecular binding models with the critical amino acids of the receptors. Dynamics performance does not display with high accuracy by using molecular docking. So, to better identify the binding modes of ligands, molecular dynamics simulations were also conducted on the structure of macromolecule.

Materials and Methods

Data set

The biological data set used in this paper was achieved from the report of Teng Yu-Ou. The data set is the anticancer properties of a novel series of 5-(2-Carboxyethenyl)-isatin against human leukemia Jurkat cells. The structural feature and antiproliferative value of these compounds were shown in Table 1. The anticancer activities were transformed into logarithmic scale (pIC_{50}) and used as the dependent variable in QSAR analysis.

Molecular descriptors

The spatial structure of compounds was drawn by

HyperChem (Hyper-cube Inc., Version 8.0.3) software [23], and Polak-Ribiere algorithm was used for optimization of the structures. Molar volume (V), molecular surface area (SA), hydrophobicity (log P), hydration energy (HE), and molecular polarizability was achieved with Hyperchem software. Also, Topological, geometrical, charge, empirical and constitutional descriptors for each molecule. 2D autocorrelations aromaticity indices, atom-centered fragments, and functional groups were generated by a Dragon program package (version 5.5) [24].

Model validation

Four different chemometrics methods including; (1) stepwise-multiple linear regression, (2) MLR with factor analysis (FA-MLR), (3) genetic algorithm-multiple linear regression (GA-MLR), and (4) genetic algorithm- partial least squares (GA-PLS) were performed. In order to validae the output equation, statistical parameters such as; correlation coefficient (R^2), leave-one-out cross-validation correlation coefficient (Q^2), cross-validation (Cvcv), variance ratio (F) standard error of the regression (SE), and root mean square error on an external set of data (R^2p) were applied.

Docking procedures

Docking procedures was executed by DOCK-FACE (*in-house* batch script) [24, 25]. Firstly, the three-dimensional crystal structure of Caspase-3 (PDB ID: 1GFW) was achieved from Protein Data Bank (PDB database; http://www.rcsb.org) [26]. Then, water molecules and co-crystal ligand were removed from protein structure. For checking missing residues, MODELLER 9.17 was used to obtian the final structure as PDB format [27]. Afterwards, the final PDB structure converted to PDBQT using MGL tools software [28]. HyperChem software package (Version 7, Hypercube Inc) was applied to create the 3D structure of molecules. Molecular Mechanic (MM^+), then semi-empirical AM1 method was performed to optimize the ligands, in the following combining non-polar hydrogen of compounds and defining rotatable bonds were accomplished. After that, 100 independent genetic algorithms (GA) method with 150 population size, 2,500,000 energy evaluations, 27,000 generations, and a gene mutation rate of 0.02 was run. A grid box of 40, 40, and 40 in x-, y-, and z directions was defined for the system and for all visualization and evaluation of interactions, VMD software and PLIP (fully automated protein–ligand interaction profiler) were used [28-30].

Molecular Dynamics Simulations

The obtained complex structures (Pro-ligand) were utilized as the input documents for MD simulation. MD was done through the GROMACS v5.0.6. Input structures were prepared by GROMOS96 53a6 as the force field. The correct situation of Histidine hydrogen was defined for all histidine inside of protein and disulfide boned.

In the next level, the surface charges of the structure were neutralized by adding Na and Cl. For definition of the grid box, the complex was located in an octahedron box. This step was operated via a steep descent algorithm during 1000 steps in order to remove the Van der Waals interactions and construct hydrogen bonds between water and complex.

In the next step, the temperature of the system increased gradually from 0 to 310 k over 200ps (volume is constant), and then, it was equilibrated in the constant pressure. Finally, MD simulation was carried in the mentioned temperature over 100ns. The trajectories of the simulations were then loaded to VMD for further analyses and visualization of the binding mode.

Results and Discussion

QSAR studies

The structural features and the anticancer activities of the tested ligands (represented as pIC_{50}) are shown in Table 1. QSAR analysis was done to understand the relationship between antiproliferative activities and
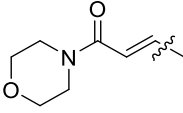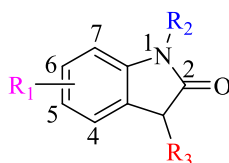

1-33; R_3: $=O$

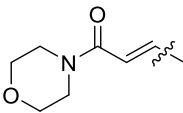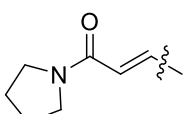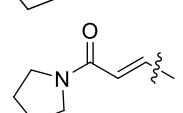34-35; R_3: $-OH$

36-37; R_3: $=NOH$

Table 1. Chemical structure, Experimental and Predicted activity by (GA-PLS) for cytotoxic activity and binding energy valuses of (5-(2-Carboxyethenyl)-isatin analogues

Entry	R_1	R_2	Exp. pIC_{50}	Pred. pIC50**	Binding Energy (kcal/mol)
1*	5-CH=CHCOOCH₃	H	---	---	---
2*	5-CH=CHCOOCH₃	CH3	---	---	---
3*	5-CH=CHCOOCH₃	CH₂CH₃	---	---	---
4	5-CH=CHCOOCH₃	CH₂C₆H₅	7.1	7.01	-8
5	5-CH=CHCOOCH₃	CH₂-(4-F-C₆H₄)	6.4	6.57	-8.2
6	5-CH=CHCOOCH₃	CH₂-(4-CN-C₆H₄)	7.09	7.11	-7.7
7	5-CH=CHCOOCH₃	CH₂-(4-CN-C₆H₄)	6.4	6.2	-8.4
8	5-CH=CHCOOCH₃	CH₂-(4-CH₃-C₆H₄)	7.3	6.99	-7.6
9	5-CH=CHCOOCH₃	CH₂-(4-OCH₃-C₆H₄)	7.52	7.69	-8.4
10	5-CH=CHCOOCH₃	CH₂-(4-Cl-C₆H₄)	6.58	6.8	-7.3
11	5-CH=CHCOOCH₃	CH₂-(3Cl-4Cl-C₆H₃)	6.07	6.2	-7.7
12**	5-CH=CHCOOCH₃	CH₂-(4-Br-C₆H₄)	6.97	7.22	-7.5
13	5-CH=CHCOOCH₃	CH₂-(3-Br-C₆H₄)	6.9	6.47	-7.4
14	5-CH=CHCOOCH₃	CH₂-(2-Br-C₆H₄)	6.09	5.78	-8.1
15**	5-CH=CHCOOCH₃	CH₂C₁₀H₇	6.1	6.2	-8.9
16	5-CH=CHCOOCH₃	CH₂CH₂OC₆H₅	6.69	6.61	-7.7
17**	5-CH=CHCOOCH₃	CH₂C₆H₃-(3,3-CH₃)	6.2	6.33	-7.8
18**	4-CH=CHCOOCH₃	CH₂-(4-OCH₃-C₆H₄)	6.1	6.21	-7.7
19	6-CH=CHCOOCH₃	CH₂-(4-OCH₃-C₆H₄)	5.5	5.68	-7.2
20**	5-CH=CHCOOC₂H₅	CH₂-(4-OCH₃-C₆H₄)	7.52	6.32	-8.6
21**	5-CH=CHCOOC₂H₅	CH₂-(4-Br-C₆H₄)	7.15	7.14	-7.6
22**	5-CH=CHCOOtBu	CH₂-(4-OCH₃-C₆H₄)	6.65	6.58	-7.5
23**	5-CH=CHCOOtBu	CH₂-(4-Br-C₆H₄)	6.15	6.16	-7.5

*: Outlier data

**: Molecules as test set

Table 1. Ctd

Entry	R$_1$	R$_2$	Exp. pIC$_{50}$	Pred. pIC50**	Binding Energy (kcal/mol)
24	5-CH=CHCOOtBu	CH$_2$-(4-OCH$_3$-C$_6$H$_4$)	6.5	6.28	-8
25	5-CH=CHCOOtBu	CH$_2$-(4-Br-C$_6$H$_4$)	5.98	6.14	-8.3
26**	CH=CHCOO(CH$_2$)$_2$OH	CH$_2$-(4-OCH$_3$-C$_6$H$_4$)	6.3	5.94	-7.6
27	5-CH=CHCOO(CH$_2$)$_2$OH	CH$_2$-(4-Br-C$_6$H$_4$)	6.39	6.5	-7.8
28	5-CH=CHCONH$_2$	CH$_2$-(4-OCH$_3$-C$_6$H$_4$)	5.76	5.94	-7.4
29	5-CH=CHCONH$_2$	CH$_2$-(4-Br-C$_6$H$_4$)	5.63	5.12	-7.6
30		CH$_2$-(4-OCH$_3$-C$_6$H$_4$)	5.34	5	-8.7
31		CH$_2$-(4-Br-C$_6$H$_4$)	5.84	5.66	-8.6
32		CH$_2$-(4-OCH$_3$-C$_6$H$_4$)	5.65	5.89	-8.4
33		CH$_2$-(4-Br-C$_6$H$_4$)	5.49	5.58	-8.5
34**	5-CH=CHCOOCH$_3$	CH$_2$-(4-OCH$_3$-C$_6$H$_4$)	7.52	7.21	-8.3
35	5-CH=CHCOOCH$_3$	CH$_2$-(4-Br-C$_6$H$_4$)	5.91	6.1	-7.6
36	5-CH=CHCOOCH$_3$	CH$_2$-(4-OCH$_3$-C$_6$H$_4$)	5.04	5.29	-7.8
37**	5-CH=CHCOOCH$_3$	CH$_2$-(4-Br-C$_6$H$_4$)	5.23	5.41	-7.9

different molecular descriptors. Five different chemometrics methods (i.e., stepwise MLR, FA-MLR, PCR, GA-MLR, and GA-PLS) were applied. The descriptors which used are shown in Table 2.

As depicted in Figure 1, a principal component analysis was performed to detect the outlier data, so molecules **1**, **2**, and **3** were omitted, and to achieve calibration and test set of data, Kennard stone algorithm was defined.

Table 3 showed the results of QSAR models,

Table 2. The Brief descriptors which used in the QSAR models

| Descriptor type	Descriptors	Brief description
3D-MORSE descriptors	Mor08v	3D-MORSE-signal08/weighted by atomic van der waals volumes
	Mor27m	3D-MORSE-signal27/weighted by atomic masses
	Mor24u	3D-MORSE-signal24/unweighted
	Mor27u	3D-MORSE-signal27/unweighted
RDF descriptors	RDF040e	Radical Distribution Function-4.0/weighted by atomic Sanderson electronegative
	RDF140m	Radical Distribution Function-140/weighted by atomic masses
Topological descriptors	PW4	Path/walk4-Randic shape index
Gateway descriptors	R5v	R autocorrelation of lag5/weighted by atomic van der waals volumes.
WHIM descriptors	E2u	2-nd component accessibility directional WHIM index unweighted
	E3u	3-nd component accessibility directional WHIM index unweighted
Geometrical descriptors	QXXm	QXX COMMA2 value/weighted by atomic masses
2D-frequency fingerprints	F02[N-O]	Frequency of N-O at topological distance 04
2D-autocorrelatin	MATS8m	Moran autocorrelation –lag8/weighted by atomic masses
Geometrical	PJI3	3D petitjean shape index
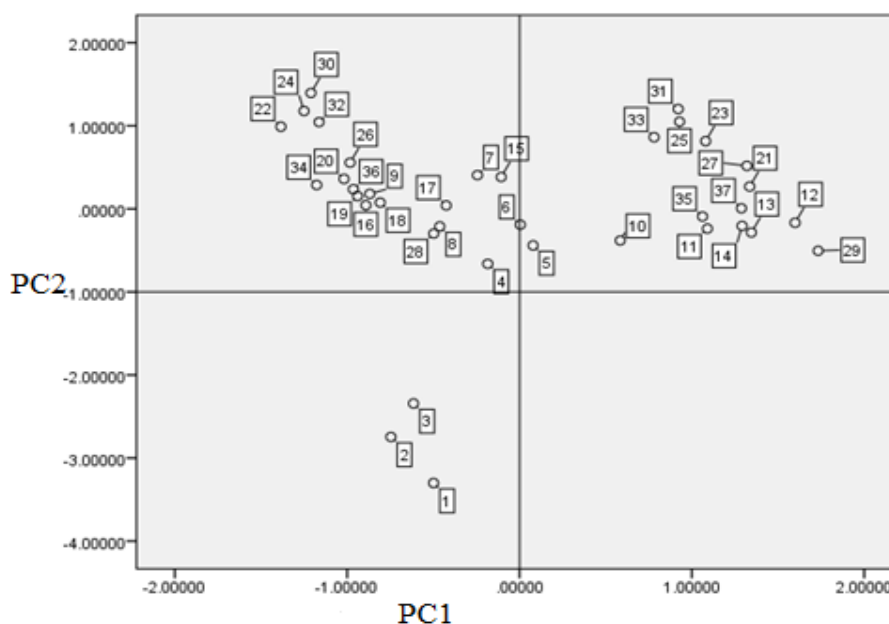
Figure 1. Outlier data diagram analysed by principal component analysis

Table 3. The results of different QSAR model analysis

Eq no.	Equation	R^2	R^2test	Cvcv	F	SE	R^2p
1. MLR	PIC_{50}=-4.6 Mor08v (±0.55)-2.5 Mor27m (±0.3)-0.1 RDF040e (±0.01)-0.4 RDF140m (±0.4)+69.9 PW4 (±14.45)-52.06 R5v (±10.6)-4.05 E2u (±1.25)+0.004 QXXm (±0.002)	0.91	0.87	3.9	38.9	0.17	0.89
2. FA_MLR	PIC_{50}=-2.98 Mor24u (±0.24) +6.76 (±0.167)	0.54	0.51	3.2	10.5	0.28	0.5
3. PCR	PIC_{50}= 0.349 PC5 (±0.084)- 0.329 PC4 (±0.082) − 0.253PC1(±0.084)+ 0.179 PC3 (±0.084) + 8.235 (±0.082)	0.84	0.79	3.6	16.75	0.39	0.78
4.GA_MLR	PIC_{50}=-2.7 Mor24u (±0.36)-1.7 Mor27u (±0.34)-0.32 F02[N-O] (±0.06)+0.73 MATS8m (±0.2) + 2.6 PJI3 (±0.87)+ 4.6 (±0.9)	0.89	0.80	4.8	29.6	0.24	0.88

whereas Equation 1 was selected as the best equation in the MLR model. The variables which were chosen in MLR equation, showed that 3D-MORSE descriptors (Mor08v, Mor27m), RDF descriptors (RDF040e, RDF140m), Topological (PW4), Gate away descriptors (R5v), WHIM descriptors (E2U), and geometrical descriptors (QXXm), affect the activity of the studied compounds. All of the descriptors used in this equation have a negative effect, except for PW4 as topological descriptor, on anticancer activity.

Equation 2, described the selected variable in FA-MLR model, Mor24u, as 3D-MORSE descriptor, affect the activity of the studied compounds. The variances of the anticancer activity, 0.54%, could be explained by the selected one factors, however, this model is not suitable for predicting variance on anticancer activity.

Eq 3, displayed the principal scores of 1, 3, 4, and 5

which are as input variables for PCR analysis. It demonestrated obviously higher calibration and lower cross-validation statistics in comparison to FA-MLR analysis, as depicted in Table 4, Principal Score 1 explained the importance of nCIR, FDI, E2u and R7u+ descriptors, Principal Score 3 signified the importance of MATS8p, QXXm, RDF085m descriptors on anticancer activity. Furthermore, Principal Score 4, displayed the importance of MATS2e and C-011 descriptors and finally Principal Score 5, indicated the importance of E3U and R5v+ descriptors. The statistical parameters of the results obtained from the GA-MLR model could explained 0.89% of the variance and predicted 80% of the variance in data ($-logIC_{50}$).

PLS analysis is better than MLR analysis due to omitted multicollinearity in the descriptors and decreased noisy data. In this method, a genetic

Table 4. Numerical values of factor loading numbers 1–6 for some descriptors after VARIMAX rotation (against anticancer activity)

	Component					
	1	2	3	4	5	6
Hyd.Egy	0.067	-0.192	-0.076	-0.175	0.066	0.720
nCIR	0.805	0.142	-0.100	-0.172	0.180	0.261
PW4	0.845	0.084	-0.243	0.180	0.137	-0.157
MATS8p	-0.098	0.235	-0.834	0.111	-0.073	0.216
MATS2e	-0.292	-0.175	0.117	-0.840	0.032	-0.145
FDI	-0.743	-0.285	-0.03	0.311	0.367	-0.131
QXXm	-0.335	0.007	0.723	0.272	0.373	0.029
RDF040e	0.589	0.679	-0.096	0.190	-0.135	0.015
RDF085m	-0.09	0.291	0.643	0.361	0.029	0.213
RDF075e	0.283	0.767	0.200	0.041	-0.125	0.024
RDF140m	-0.254	0.470	-0.416	-0.565	0.232	0.054
RDF105e	-0.05	0.178	-0.01	0.255	-0.298	0.708
Mor08v	0.059	0.231	0.480	0.576	0.415	-0.247
Mor27m	0.163	0.239	-0.549	-0.038	-0.327	0.025
Mor24u	0.051	0.759	0.172	0.400	0.033	-0.102
E2u	0.714	0.107	0.235	-0.019	-0.419	-0.02
E3u	-0.019	-0.044	-0.239	0.022	-0.839	0.137
R7U+	-0.709	-0.551	0.005	-0.062	0.130	0.042
R5V+	-0.291	-0.389	0.344	0.163	0.706	0.083
R6e	0.497	-0.251	-0.280	0.061	-0.123	-0.304
C-011	-0.088	0.142	0.166	0.840	0.077	-0.072

algorithm was selected to find the more adequite set of descriptors. To realize the optimum number of latent variables, the leave-one-out cross-validation method was executed for each PLS model,

Figure 2, showed a combination of Topological (PW4), RDF descriptors (RDF040e and RDF140m), 3D-MORSE descriptors (Mor08v, and Mor27m), WHIM (E3u), and Gateway descriptors (R5v) have been chosed by GA-PLS to account for anticancer activity of isatin derivatives and six of them obtained by MLR analysis. Furthermore, E3u and PW4, had a positive coefficient on the anticancer activity, while the other descriptors had a negative effects. In GA-MLR, the combination of topological, geometrical, and 3D-Morse descriptors, made the relationship between the structure and activity of the studied isatin derivatives. The MATS8m as 2D-autocorrelation descriptors, addressed the topology of the structure or parts there of in
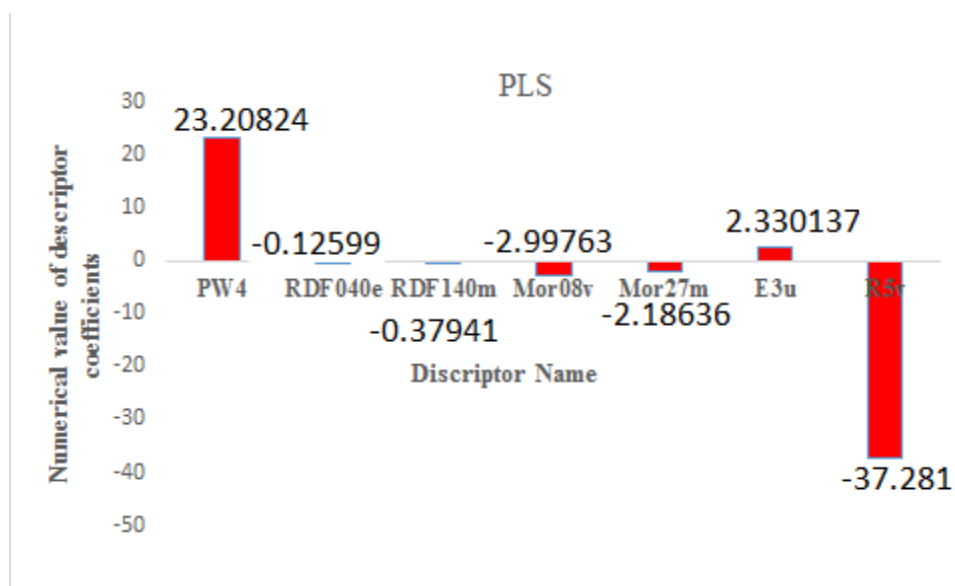
Figure 2. PLS regression coefficients for the variables used in GA-PLS model.

connection with a particular physicochemical property. 3D-MoRSE descriptors such as Mor24u and Mor27u, were very versatile 3D structure encoding framework and showed details on the whole molecular structure of isatin compounds. PJI3 (3D Petitjean shape index) is among the geometrical descriptors. The GA-PLS model indicated a high statistical quality $R^2 = 0.91$ and $Q^2 = 0.81$. The predictive ability of the model was measured by applying this model to 11 external test set molecules. The squared correlation coefficient for prediction was 0.92, and the standard error of prediction was 0.49. Figure 3 showed the plots of linear regression predicted versus the experimental value of the cytotoxic activity of molecule. The plots for this model showed to be more apporopriate with $R^2cv= 0.81$.

To understand the relative importance of the variable which appeared in a PLS model, Variable Important in Projection (VIP), was used According to Erikson et al (Fig. 4). VIP showed, PW4, as Topological descriptor, and R5v as Gateway descriptor, are the most critical indices in the QSAR equation derived by PLS analysis. Besides, the other descriptors were low influential parameters [31].

To determine, Robustness and applicability domain of the models, Leverage method was used. The calculated leverage values of the test set samples for all models and the warning leverage, as the threshold value for accepted prediction, were showed in Table S1. As seen, the leverages of all test samples are lower than $h*$ for all models. This means that all predicted values are
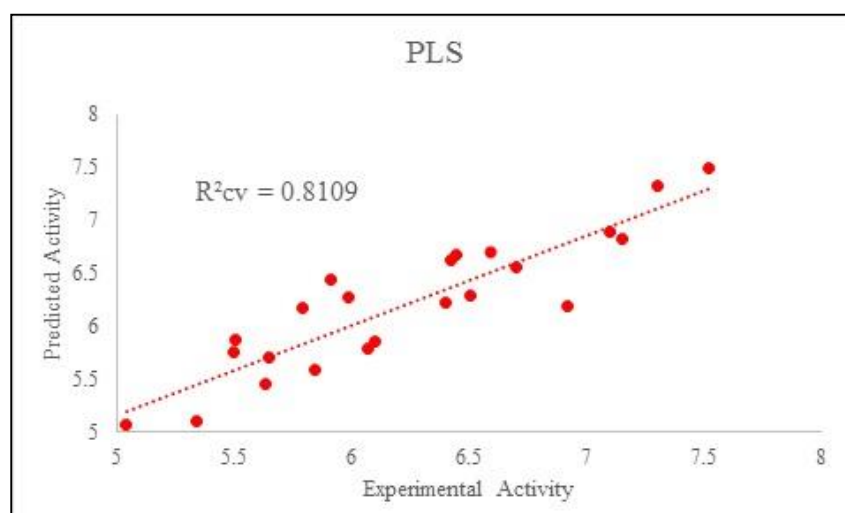

Figure 3. The Plot of the cross-validated predicted activity against the experimental activity for the QSAR models obtained by GA-PLS methods.
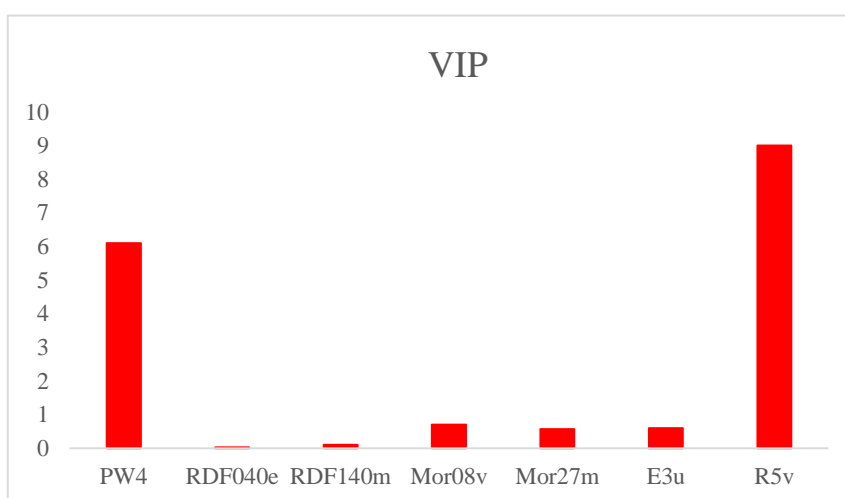

Figure 4. The Plot of variables important in projection (VIP) for the descriptors used in the GA-PLS model.

acceptable.

Docking Study

Molecular modeling was carried out to predict the binding mode of these molecules with the target enzyme (PDB ID: 1GFW). All the docking protocols were done on validated structures with RMSD values 2 Å. The conformation with the lowest binding energy was considered as the best docking result. The binding energies of all compounds were reported in Table 1. Comparing these energies to its corresponding one (-8.7 (Kcal/mol)) for co-crystal ligand showed that compounds **15**, **30**, and **31** represented better binding than the co-crystal ligand (MSI). As depicted in Figure 5, the oxygen atom attached to C3 position of isatin in compound **15,** was involved in hydrogen-bonding interactions with Ser209 and Asn 208. Also some hydrophobic interaction with the residue Tyr 204, Trp 206, Trp 214, and Phe 256 were observed. Morever, acceptor hydrogen bonds existed between the oxygen of morpholine ring with Arg 207. The phenoxy ring attached to isatin ring is also involved in hydrogen bonding interaction with Phe 250 in compound 30. Furthermore, the isatin ring formed pi-stacking interaction with Trp 206 and there were some hydrophobic interactions through Trp 206, Trp 214 and Phe 256. To explain the binding mode of compound **31**; there were hydrogen bond interaction between oxygen atom attached to C_3 position of isatin and Ser 209, pi-stacking between isatin ring and Trp 206 and also some hydrophobic interaction with the residue of Trp 206 and Phe 256. The two key interactions of co-crystal ligand (MSI) included two hydrogen bonds between sulfonyl group of co-crystal ligand and Arg 207, and also carbonyl group of isatin ring with Ser 120, Gly 122 and Cys 163 and hydrophobic interactions with Tyr 204 and Phe 256. The result obtained from the docking study indicated that the main interaction of tested compounds was actually H-bond formation of oxygen atom of C_3 of isatin with Ser 209 which was a critical amino acid in the active site of the target.
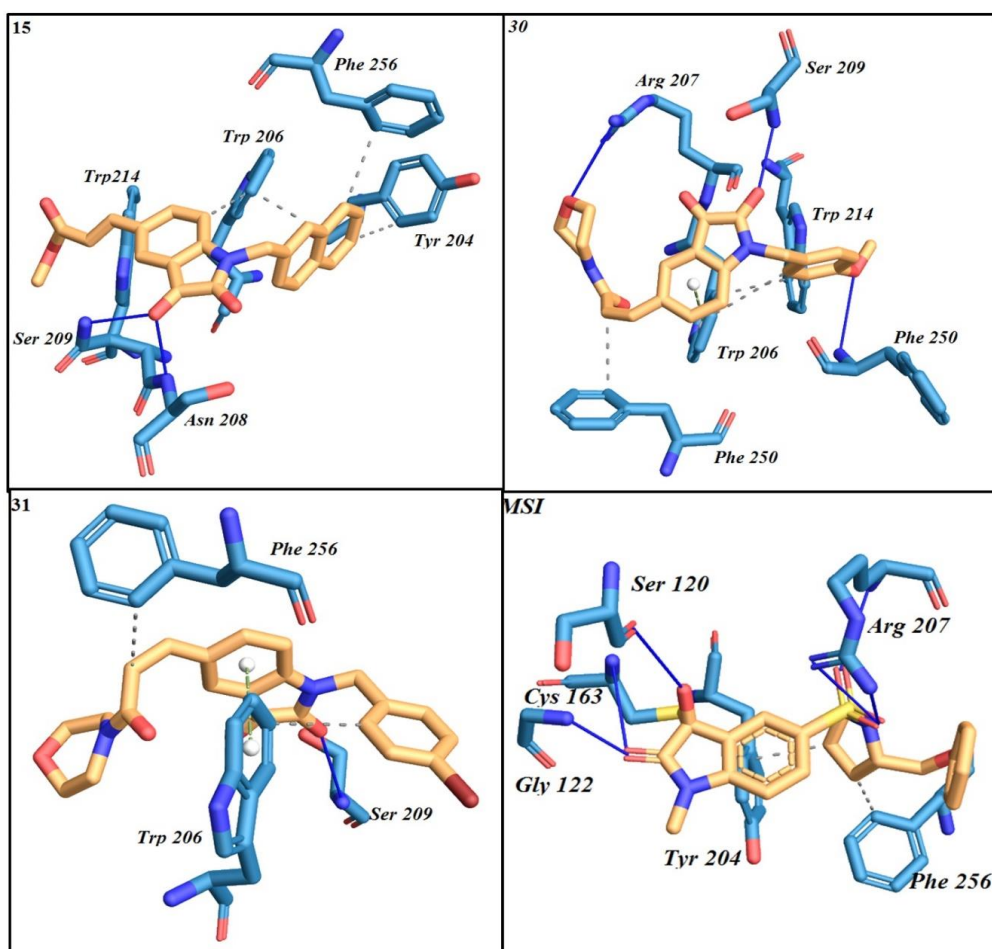

Figure 5. Interactions of **15**, **30**, **31** and MSI with the residues in the binding site of the receptor (1GFW).

Molecular Dynamics Simulations

Firstly, according to the energy diagram of the system, the equilibration phase was done successfully (Fig. 6A). After preforming molecular dynamics simulation during 100 ns and reaching an equilibrate system based on RMSD variation, a steady-state established after 80 ns from the beginning of the simulation. Calculation of RMSD was used to obtain the conformational stability of the complex during this simulation. As could be seen, about 75 ns after starting point, RMSD reached below 2nm and then leveled off for the complex (Fig. 6B).

The root-mean-square fluctuation (RMSF) describes the ratio of positional variety of a given atom over time. Although RMSF, as well as RMSD, are mathematical measurements, RMSF measuring individual residue flexibility, or how much a particular residue moves (fluctuates) during a simulation instead of indicating positional differences between entire structures over time. RMSF per residue was sketched vs. residue number and can show structurally which amino acids in a protein contributed the most to molecular motion. Based on the RMSF curve and Heatmap plot, residue no. 200-210, 250-260, 120-122 contributed to the binding of active site (Fig. 7).

Conclusion

To interprte of anticancer activity and also establish the QSAR model for investigated isatin derivatives, we used five distinct methods including; MLR, FA-MLR, PCR, GA-MLR, and GA-PLS. Based on the generated QSAR models, GA-PLS and MLR, displayed desirable results for predicting the pIC_{50} of isatin analogous. The GA-PLS model possessed higher predictive ability by the cross-validation methods. This study proffered the significance of Topological, RDF, 3D-MORSE, WHIM, Gateway descriptors which are related to tested isatin derivatives in order to design new and potent compounds. Docking study revealed that, all the studied compounds interacted with Ser209 and Phe256 as the
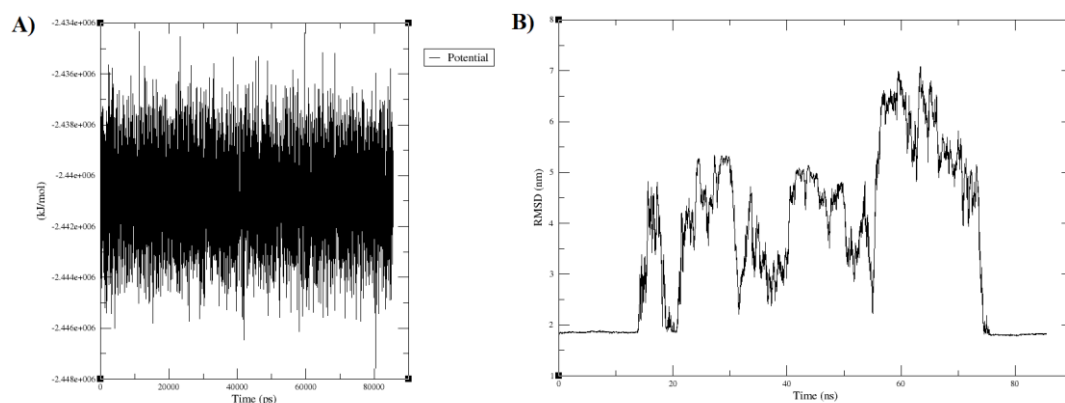

Figure 6. A) Potential Energy curve during 100 ns simulation. B) RMSD curve during 100 ns simulation
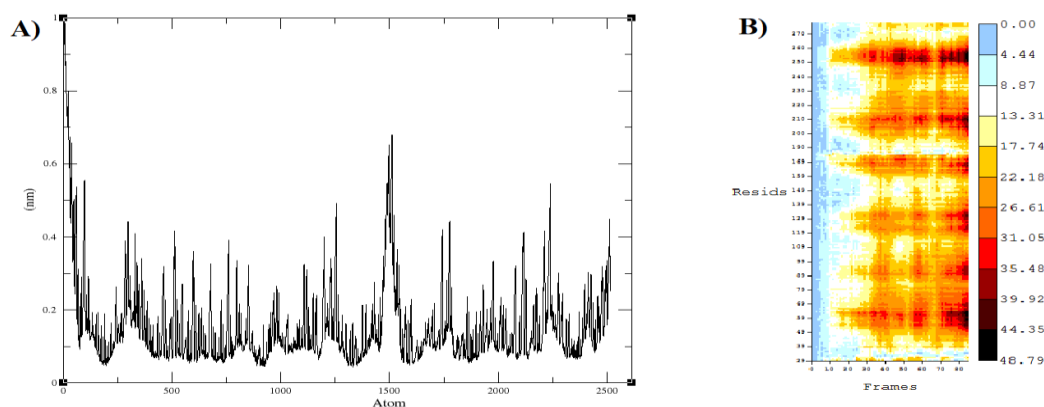

Figure 7. A) RMSF curve. B) Heatmap Plot

key amino acids of the active site, through hydrogen-bond interactions by oxygen atom at C_3 position of isatin ring. According to dynamic simulation's result, there was an appropriate interaction between compound **15** and protein. Indeed, These two matched up perfectly during the 100 ns of simulation.

Acknowledgements

References

1. Veneis P, Wild CP. Causes and prevention, Wild CP Global cancer patterns. Lancet. 2013;32(4):465-78.

2. Thun MJ, DeLancey JO, Center MM, Jemal A, Ward EM. The global burden of cancer: priorities for prevention. Carcinogenesis. 2010;31(1):100-10.

3. Boyle P LB. World cancer report. RC Press. International Agency for Research on Cancer. 2008.

4. Chopra R, Lopes G. Improving access to cancer treatments: the role of biosimilars. J Glob Oncol. 2017;3(5):596-610.

5. Gangarapu K, Thumma G, Manda S, Jallapally A, Jarapula R, Rekulapally S. Design, synthesis and molecular docking of novel structural hybrids of substituted isatin based pyrazoline and thiadiazoline as antitumor agents. Med Chem Res. 2017;26(4):819-29.

6. Thadhaney B, Sain D, Pemawat G, Talesara GL. Synthesis and antimicrobial evaluation of ethoxyphthalimide derivatized spiro [indole3,5′-(1,3)thiazolo(4,5-c)isoxazol]-2(1H)-ones via ring closure metathesis. Indian J Chem B. 2010;49: 368-373.

7. Dmytro H, Borys Z, Roman L. Synthesis, Biological Activity of Thiazolidinones Bearing Indoline Moiety and Isatin Based Hybrids. Mini Rev Org Chem. 2015;12(1):66-87.

8. Havrylyuk D, Zimenkovsky B, Vasylenko O, Gzella A, Lesyk R. Synthesis of New 4Thiazolidinone-, Pyrazoline-, and Isatin-Based Conjugates with Promising Antitumor Activity. J Med Chem. 2012;55 (20):8630-8641.

9. Liang C, Xia J, Lei D, Li X, Yao Q, Gao J. Synthesis, in vitro and in vivo antitumor activity of symmetrical bis-Schiff base derivatives of isatin. Eur J Med Chem. 2014;74:742-750.

10. Huong TT, Dung do TM, Oanh DT, Lan TT, Dung PT, Loi VD. 5-aryl-1,3,4thiadiazole-based hydroxamic acids as histone deacetylase inhibitors and antitumor agents: synthesis, bioevaluation and docking study. Med Chem Shariqah (United Arab Emirates). 2015;11(3):296-304.

11. Lesyk R HD, Lelyukh M. Synthesis and anticancer activity of isatin, oxadiazole and 4thiazolidinone based conjugates. Chem Chem Technol. 2015;9(1):29-36.

12. Varma RS, Khan IA. Potential biologically active agents. X. Synthesis of 3-arylimino-2indolinones, and their 1-methyl- and 1-morpholino/piperidinomethyl derivatives as excystment and cysticidal agents against Schizopyrenus russelli, Pol J Pharmacol Pharm.1977;29(5):549-54.

13. Socca EA, Luiz-Ferreira A, de Faria FM, de Almeida AC, Dunder RJ, Manzo LP. Inhibition of tumor necrosis factor-alpha and cyclooxigenase-2 by Isatin: a molecular mechanism of protection against TNBS-induced colitis in rats. Chem Biol. 2014;209:48-55.

14. Rad MNS, Behrouz S, Nekoei AR, Faghih Z, Khalafi-Nezhad A. Three-component synthesis of some novel N-heterocycle methyl-O-oxime ethers. Synthesis. 2011;2011(24):4068-76.

15. Medvedev A, Buneeva O, Glover V. Biological targets for isatin and its analogues: Implications for therapy, Biologics. Targets Ther. 2007;1(2):151-162.

16. Zhou L, Liu Y, Zhang W, Wei P, Huang C, Pei J. Isatin compounds as noncovalent SARS coronavirus 3C-like protease inhibitors, J Med Chem. 2006;49(12):3440-3443.

17. Chapman JG, Magee WP, Stukenbrok HA., Beckius GE., MiliciA J. A novel nonpeptidic caspase-3/7 inhibitor. (S)-(+)-5-[1-(2-methoxymethylpyrrolidinyl) sulfonyl] isatin reduces myocardial ischemic injury. Euro J Pharm. 2002;456(3):59-68.

18. Cao J, Gao H, Bemis G, Salituro F, Ledeboer M, Harrington E. Structure-based design and parallel synthesis of N-benzyl isatin oximes as JNK3 MAP kinase inhibitors. Bioorg Med Chem Lett. 2009;19(10):2891-2895.

19. Cane A, Tournaire MC, Barritault D, Crumeyrolle-Arias M. The endogenous oxindoles 5-hydroxyoxindole and isatin are antiproliferative and proapoptotic. Biochem Bioph Res Co. 2000;276(1):379-384.

20. Fereidoonnezhad M, Faghih Z, Mojaddami A, Rezaei Z, Sakhteman A. A comparative QSAR analysis, molecular docking and PLIF studies of some N-arylphenyl-2, 2-dichloroacetamide analogues as anticancer agents. Iran J Pharm Res. 2017;16(3):981.

21. Hemmateenejad B, Emami L, Sharghi H. Multi-wavelength spectrophotometric determination of acidity constant of some newly synthesized Schiff bases and their QSPR study. Spectrochim Acta A. 2010;75(1):340–346.

22. Teng YO, Zhao HY, Wang J, Liu H, Gao ML, Zhou Y. Synthesis and anti-cancer activity evaluation of 5-(2-carboxyethenyl)-isatin derivatives. Eur J Med Chem. 2016;112:145-56.

23. Teng YO, Zhao HY, Wang J, Liu H, Gao ML, Zhou Y. Synthesis and anti-cancer activity evaluation of 5-(2-carboxyethenyl)-isatin derivatives. Eur J Med Chem. 2016;112:145-156.

24. Fereidoonnezhad M, Faghih Z, Mojaddami A, SakhtemanA , Rezaei Z. A comparative docking studies of dichloroacetate analogues on four isozymes of pyruvate dehydrogenase kinase in humans. Indian J Pharm Educ.2016;50(4):S32-S8.

25. Fereidoonnezhad M, Tabaei SMH, Sakhteman A, Seradj H, Faghih Z. Design, synthesis, molecular docking, biological evaluations and QSAR studies of novel dichloroacetate analogues as anticancer agent. J Mol Struc. 2020;1221:128689

26. R. Leardi. Application of genetic algorithm–PLS for feature selection in spectral data sets. J Chemom. 2000;14(5):643-655.

27. Emami L, Sabet R, Sakhteman A, Khoshnevis Zadeh M.

Quantitative Structure–Activity Relationship and Molecular Docking Studies of Imidazolopyrimidine Amides as Potent Dipeptidyl Peptidase-4 (DPP4) Inhibitors. J Pharm Res Int. 2019;27(6):1-15.

28. Zare S, Fereidoonnezhad M, Afshar D, Ramezani Z. A comparative QSAR analysis and molecular docking studies of phenyl piperidine derivatives as potent dual NK1R antagonists/serotonin transporter (SERT) inhibitors. Comput Biol Chem. 2017;67:22-37.

29. Emami L, Faghih Z, Sakhteman A, Rezaei Z, Faghih Z, Salehi F, et al. Design, synthesis, molecular simulation, and biological activities of novel quinazolinone-pyrimidine hybrid derivatives as dipeptidyl peptidase-4 inhibitors and anticancer agents. New J Chem. 2020;44(45):19515-31.

30. Salentin S, Schreiber S, Haupt VJ, Adasme MF, Schroeder M. PLIP: fully automated protein-ligand interaction profiler. Nucleic acid res. 2015;43(W1):W443- W447.